24th Australasian Fluid Mechanics Conference - AFMC2024
Canberra, Australia
1-5 December 2024
Paper No: AFMC2024-75

Wind Turbine/Farm Simulations Using an Immersed Boundary Method

Jack Park[1,2*], Daniel Linton[2] and Ben Thornber[2,3]

[1] Institute of Software Methods for Product Virtualization, German Aerospace Center (DLR), Dresden SN 01069, Germany
[2] School of Aerospace, Mechanical and Mechatronic Engineering, The University of Sydney, Sydney NSW 2006, Australia
[3] School of Mechanical and Aerospace Engineering, Queen's University Belfast, Belfast NIR BT7 1NN, The United Kingdom
*Email: jack.park@dlr.de

1 Introduction

Detached eddy simulations of wind turbine/farm are conducted, where the nacelle and tower are represented by the immersed boundary method (IBM), and the unsteady wind turbine blades are modelled by the actuator surface model (ASM). The solver (Park *et al.*, 2020) provides significant advantages over the conventional body-fitted mesh approach in terms of the computational cost because the relative motion between the rotating and non-rotating components can be resolved without any mesh deformation.

The IBM-ASM solver has been initially developed for rotorcraft aerodynamics simulations, and it has been comprehensively validated for several different helicopter configurations (Park *et al.*, 2020). The aim of this research is to expand the area of applications to wind energy.

The first validation case considered in this study is a single New MEXICO wind turbine in a uniform flow with two different yaw angles (0 and 30 degrees) at three different tip-speed ratios (Boorsma *et al.*, 2018). Secondly, a single model wind turbine in an atmospheric boundary layer (ABL) is studied using the concurrent inflow approach. Lastly, a wind farm composed of the 30 model wind turbines (Wu & Porté-Agel, 2013) is investigated.

2 Results and Discussion

In figures 1(a) and 1(b), the drag and power coefficients from the New MEXICO single wind turbine simulations (axial flow) are presented, respectively. The outcomes show that the IBM-ASM solver has closer agreement to experiment than TAU-URANS body-fitted grid computations. Figure 1(c) shows a close-up of the nested grid for the ASM, and the instantaneous snapshot of the Q-criterion from the yawed flow simulation.

Figures 2(a)-(c) provide velocity profiles from single model wind turbine simulations at different stations. $x/R = -1$ indicates the ABL inflow profile; $x/R = 2$ is the velocity profile at an immediate downstream of the wind turbine blade; $x/R = 20$ is the far-wake profile. The simulation outcomes have excellent agreement with the experimental data, except for the hub region in figure 2(b). This is due to that the simulation didn't include the tower and nacelle, hence there is the evident discrepancy in the velocity deficit, which is recovered in the further downstream.

Lastly, figure 3 presents the top view of the velocity magnitude field from the wind farm simulation. It demonstrates the wake interactions between wind turbines in an aligned array. Note that this is also an isolated rotor simulation. In the accompanying presentation, quantitative comparisons will also be discussed.

3 Conclusions

It has been demonstrated that the IBM-ASM solver can produce simulation results with competitive accuracy compared to the high-fidelity, body-fitted URANS results. As a mid-fidelity tool, it is expected that the IBM-ASM solver can be a new, accurate, cost-efficient alternative to the high-fidelity simulations rather than low-fidelity modelling approaches, providing an equivalent level of accuracy to the high-fidelity approaches.

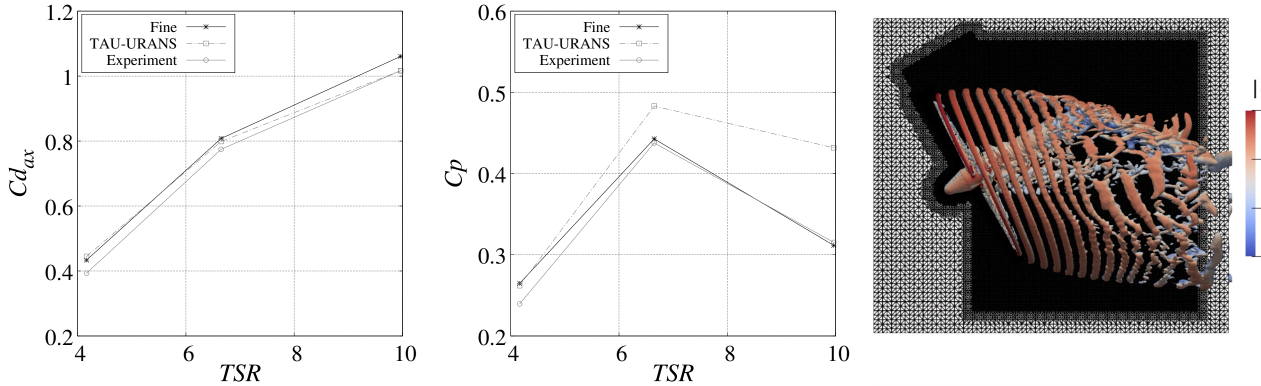

(a) Drag coefficient

(b) Power coefficient

(c) Instantaneous contour of Q-criterion

Figure 1. New MEXICO single wind turbine simulation results; Fine: IBM-ASM fine grid; TAU-URANS and Experiment from Boorsma *et al.* (2018).

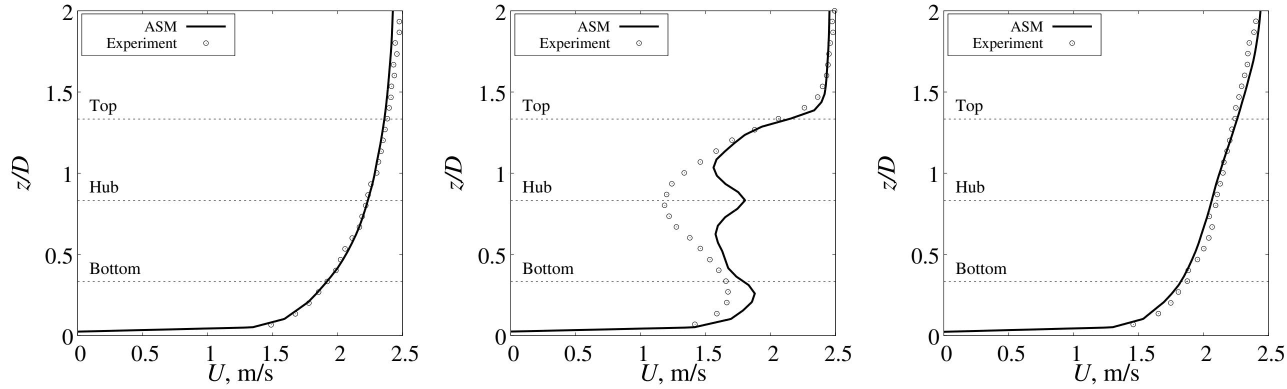

(a) Inflow profile ($x/R = -1$)

(b) Near-wake profile ($x/R = 2$)

(c) Far-wake profile ($x/R = 20$)

Figure 2. Velocity profiles from single model wind turbine simulations.

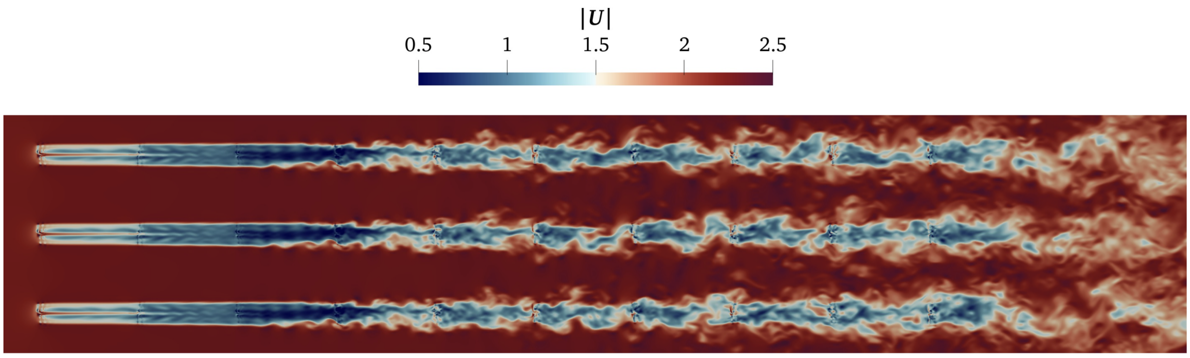

Figure 3. Top view of the velocity magnitude field from the wind farm simulation.

References

Boorsma, K., Schepers, J., Gomez-Iradi, S., Herraez, I., Lutz, T., Weihing, P., Oggiano, L., Pirrung, G., Madsen, H., Shen, W., Rahimi, H. and Schaffarczyk, P. 2018, Final Report of IEA Wind Task 29 Mexnext (Phase 3), *Technical Report ECN-E No. 18-003*, ECN.

Park, J.H., Linton, D. and Thornber, B. 2020, Towards Detached-Eddy Simulation of Flow Around Rotorcraft Using Immersed Boundary Method, *AIAA J.*, **58**(11), 4893–4907.

Wu, Y-T. and Porté-Agel, F. 2013, Simulation of Turbulent Flow Inside and Above Wind Farms: Model Validation and Layout Effects, *Boundary-Layer Meteorol.*, **146**, 181–205.